Journal of Marine Science and Technology

Volume 19 | Issue 1 Article 4

BEHAVIOR OF CATIONS IN MORTAR UNDER ACCELERATED LITHIUM MIGRATION TECHNIQUE CONTROLLED BY A CONSTANT VOLTAGE

Chih-Chien Liu
Department of Civil Engineering, ROC Military Academy, Fengshan 83059, Taiwan, R.O.C.

Wei-Chien Wang
Department of Civil Engineering, Chung Yuan Christian University, Chung Li 32023, Taiwan, R.O.C.,
a654.joy@msa.hinet.net

Chau Lee
Department of Civil Engineering, National Central University, Jhongli 32001, Taiwan, R.O.C.

Recommended Citation

Liu, Chih-Chien; Wang, Wei-Chien; and Lee, Chau (2011) "BEHAVIOR OF CATIONS IN MORTAR UNDER ACCELERATED LITHIUM MIGRATION TECHNIQUE CONTROLLED BY A CONSTANT VOLTAGE," *Journal of Marine Science and Technology*: Vol. 19: Iss. 1, Article 4.
DOI: 10.51400/2709-6998.2134
Available at: https://jmstt.ntou.edu.tw/journal/vol19/iss1/4

BEHAVIOR OF CATIONS IN MORTAR UNDER ACCELERATED LITHIUM MIGRATION TECHNIQUE CONTROLLED BY A CONSTANT VOLTAGE

Acknowledgements

The authors would like to thank the National Science Council of Taiwan for financial support of this research under Contract No. NSC 96-2221-E-008-085-MY3.

BEHAVIOR OF CATIONS IN MORTAR UNDER ACCELERATED LITHIUM MIGRATION TECHNIQUE CONTROLLED BY A CONSTANT VOLTAGE

Chih-Chien Liu*, Wei-Chien Wang**, and Chau Lee***

Key words: alkali-silica reaction, electrochemical technique, mortar, migration coefficient.

ABSTRACT

The Accelerated Lithium Migration Technique (ALMT) is an electrochemical method to remove Na^+ and K^+ from concrete, and simultaneously drive Li^+ into concrete to inhibit alkali-silica reaction (ASR). This study investigates the relationship between the applied voltage and the migration behavior of cations related to ASR. The results show that after the completion of Na^+ and K^+ removal, migration of Li^+ begins to enter a steady state. With the increase in applied voltage, the removal rate and removable amount of alkalis increases, the required time of alkalis removal and the time for Li^+ to pass through the specimen decreases, and the migration coefficients of Li^+ increase. Furthermore, the above migration parameters of cations have positive linear relationships with the average current density. After the ALMT process, the average Li/(Na + K) molar ratio of the specimen is sufficiently large to mitigate ASR problems.

I. INTRODUCTION

Remedies for alkali-silica reaction (ASR) problems include waterproofing and lithium solution impregnation methods. The former prevents water absorption and expansion of the alkali-silica gel. The latter impregnates concrete with lithium solution by spraying, soaking, or applying pressure [3, 7] to change the properties of the alkali-silica gel [9, 11]. However, ASR damage may occur again due to ineffective waterproofing. An effective depth of lithium solution impregnates into concrete through spraying and soaking only on the surface of the concrete. Driving lithium solution into concrete by pressure cannot remove the alkalis that cause the reaction.

The concept of using electrochemical methods to impregnate concrete with lithium to inhibit ASR was first suggested in 1992 by Page [8], who thought that a lithium solution could be used as an electrolyte in an electrochemical chloride extraction (ECE). Therefore, an electric field was used to impregnate concrete with Li^+. In 1996, Stokes [10] attempted to add a lithium compound to the electrolyte, then applying an electric field to impregnate concrete with Li^+. In 2000, Whitmore and Abbott [7, 13] used this method in a field application for bridge treatment. The applied DC voltage was less than 40V from the surface anode to the steel cathode. They found that the rate of Li^+ ions that migrated into the bridge deck and pier was 4-10 times faster than the soaking method to attain the same depth. Even though the use of an electrochemical technique on practical repair has already been validated [7, 13], the migration theory of cations under an electric field has not yet been established.

In 1998, the authors conceived of utilizing the characteristic of ionic migration to drive Na^+ and K^+ out of concrete, while simultaneously driving Li^+ into concrete. Experimentation showed that this method can indeed remedy ASR damage [2]. The method was subsequently named the Accelerated Lithium Migration Technique (ALMT) [6]. The effectiveness of the ASR repair is related to the amount of Li^+, Na^+, and K^+ within the specimen after repair. If the migration behavior of cations, within concrete under different electric field conditions, can be understood prior to field application, the needed parameters of maintenance can be obtained for use in field applications.

The purpose of this research was to analyze the relationship between the applied constant voltages and the migration parameters of cations within the specimen under ALMT. The parameters include: the removal rate, the removed amount and the required time for complete removal of Na^+ and K^+ out of the specimen, the time required for Li^+ to pass through the specimen, and the migration coefficient during the non-steady

Paper submitted 09/04/09; revised 10/16/09; accepted 12/21/09. Author for correspondence: Wei-Chien Wang (e-mail: a654.joy@msa.hinet.net).
**Department of Civil Engineering, ROC Military Academy, Fengshan 83059, Taiwan, R.O.C.*
***Department of Civil Engineering, Chung Yuan Christian University, Chung Li 32023, Taiwan, R.O.C.*
****Department of Civil Engineering, National Central University, Jhongli 32001, Taiwan, R.O.C.*

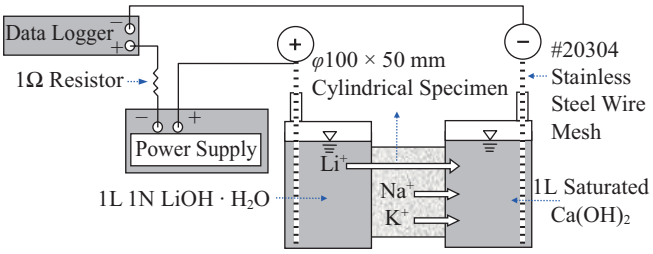

Fig. 1. Schematic diagram of the ALMT electrochemical module.

state and steady state of Li^+. In addition, the amount of cations in the specimen was analyzed after the process, thus we can validate the effectiveness of the repair.

II. EXPERIMENTAL PROGRAM

1. Materials and Specimen Preparation

ASTM Type I Portland cement was used, with an alkali content of 0.5% Na_2O_{eq} (0.11% and 0.59% for Na_2O and K_2O, respectively). Meta sandstone from eastern Taiwan was used as the aggregate. The 14-day expansion under the ASTM C1260 test was 0.033%, the 3-month expansion under the ASTM C227 test was 0.068%, and the ASTM C289 test results all determined that the aggregate has ASR potential reactivity.

Cylindrical mortar specimens of Φ 10 × 25 cm were cast, with an aggregate/cement ratio of 2.25 and a water/cement ratio of 0.5. The gradation of the fine aggregate agreed with the ASTM C227 specifications. NaOH was used to adjust the alkali content of the cement to 2.0% Na_2O_{eq}, and the total amount of Na_2O_{eq} in a specimen before the ALMT process was 11.37 kg/m^3. The specimen was cured in a 23°C, 100% R.H. environment for 3 months.

2. Apparatus and Procedure

The ALMT electrochemical module is shown in Fig. 1. The electrolytic cell has a capacity of 1 liter. 1N LiOH · H_2O and saturated $Ca(OH)_2$ were used as the anolyte and catholyte, respectively, based on prior research [2, 6], 304 stainless steel electrodes with a mesh number of 20 were used as electrodes. A data logger was used to record the changes in voltage and current during the ALMT process, while an Ion Chromatograph (IC) was used to analyze the concentrations of cations in the catholyte periodically. Changes in temperature were measured manually.

After the specimen was cured, a 5 cm-tall specimen was cut from the central portion of the cylinder. The specimen was prepared according to the ASTM C1202 before the ALMT experiment. Constant voltages of 12, 18, 24, 30, and 40 V were chosen for the ALMT experiment, assigned as V12, V18, V24, V30, and V40, respectively. The time of the process was based on the flux of Li^+ attained at a steady state. Therefore, the higher voltage case of V40 had a shorter process of 798 hours, while the rest all had a process of 1,189 hours in duration.

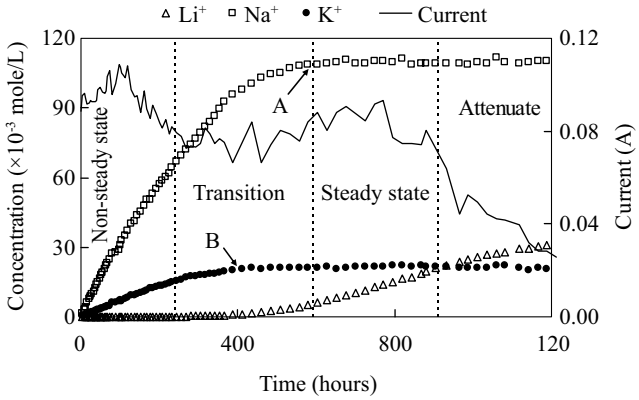

Fig. 2. Typical curves for the cation concentrations in the cathodic cell and the current varied with time during the ALMT experiment.

Each set of data in discussion is the average of two individual experimental results.

After the ALMT process, the specimen was dry cut every 5 mm starting from the anode to the cathode. Soluble ions in the slices were extracted according to the AASHTO T260 procedure. Then the Li^+, Na^+, and K^+ contents in the powder were analyzed by IC.

III. RESULTS AND DISCUSSION

1. Migration Behavior of Cations

Figure 2 shows the typical curves for the case of V30, between the cation concentrations in the cathodic cell and the current varied with time during the ALMT experiment. Removal of Na^+ and K^+ under the effect of an electric field was increased until most of the removable alkalis were removed from the sample. The figure shows that the Li^+ migration curve can be divided into four stages including non-steady state, transition, steady state, and attenuation. During the non-steady state, Na^+ and K^+ were removed from the specimen, and the current was increased first, then decreased. Li^+ migrated to the saturated pores in the specimen and had not yet arrived at the cathodic cell. During the transitional stage, the foremost Li^+ had penetrated the specimen, and the Li^+ flux in the cathodic cell increased. The removal of Na^+ and K^+ was completed (points A and B). During the steady state, the current was steadier, allowing a constant Li^+ flux. During the attenuation stage, the current gradually decreased, thus decreasing the Li^+ flux.

2. Changes in Temperature, Current, and System Resistance

Figure 3 shows that the average temperature of the cathodic cell during the ALMT experiment increased with the increase of applied voltage. Figure 4(a) shows that the current decreased with time during the ALMT experiment under the effects of constant voltage. While Fig. 4(b) shows that the system resistance, obtained by dividing the voltage by the

Table 1. Results obtained from the Na^+ and K^+ concentration-time curve in catholyte.

Experiment #	Voltage (V)	Removal Time (h)		Removal Amount ($\times 10^{-3}$ mole)[a]		Removal Percentage[b]		Alkalis Removal Percentage[c]	Average Removal Rate ($\times 10^{-3}$ mole/h)[d]	
		t_{Na}	t_K	Na^+	K^+	Na^+	K^+		v_{Na}	v_K
V12	12	1133.4	876.5	87.2	19.1	75.2	68.9	73.6	0.08	0.02
V18	18	912.4	552.7	104.8	21.5	90.3	77.6	87.4	0.11	0.04
V24	24	632.4	483.3	107.4	21.3	92.6	76.9	89.2	1.17	0.04
V30	30	572.7	388.0	108.8	21.4	93.8	77.1	90.2	0.19	0.06
V40	40	255.8	196.5	108.5	21.9	93.5	79.0	90.3	0.42	0.11

Note: [a] The total amounts of Na^+ and K^+ within a specimen are 116.0×10^{-3} and 27.7×10^{-3} mole, respectively.

[b] The removal percentage of Na^+ and K^+ is the removal amount/total amount × 100.

[c] The alkali removal percentage is

$$\frac{(Na^+ \text{ removal percentage} \times Na_2O \text{ content} + K^+ \text{ removal percentage} \times K_2O \text{ content transformed into } Na_2O_{eq})}{\text{total } Na_2O_{eq} \text{ of specimen}} \times 100,$$

where the Na_2O content is 1.61%, K_2O content transformed into Na_2O_{eq} is 0.39%, and the total Na_2O_{eq} of the specimen is 2.0%.

[d] Removal amount/removal time.

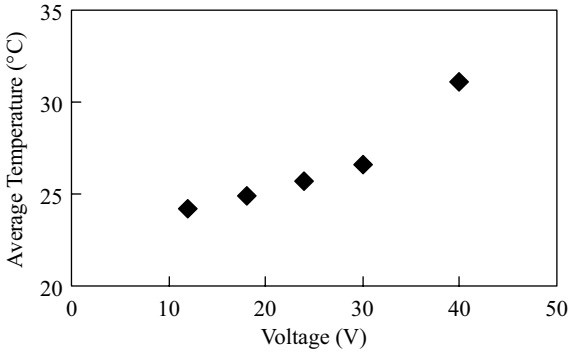

Fig. 3. Relationship between the average temperature of the cathodic cell and the applied voltage.

current during the ALMT process, increased with time. Furthermore, the current in Fig. 2 was affected by the resistance change of the specimen.

3. Migration Behavior of Na^+ and K^+

The removal time of Na^+ and K^+, denoted by t_{Na} and t_K, respectively, are obtained from points A and B in Fig. 2. The removal amount, removal percentage and the average removal rate of Na^+ and K^+, and the percentage of total alkalis removed are listed in Table 1.

The removal time of Na^+ and K^+ decreased with the increase in the applied voltage. For experiments under the same voltage, the removal time of K^+ is shorter than Na^+. This phenomenon agrees with the higher mobility of K^+ than Na^+ under the effect of an electrical field [12]. The removal percentage of Na^+ is 75.2-93.8%, while the removal percentage of K^+ is 68.9-79.0%, both increase with the increase of applied voltage. The higher removal percentage of Na^+ may result from the external addition of Na^+, which may not be combined

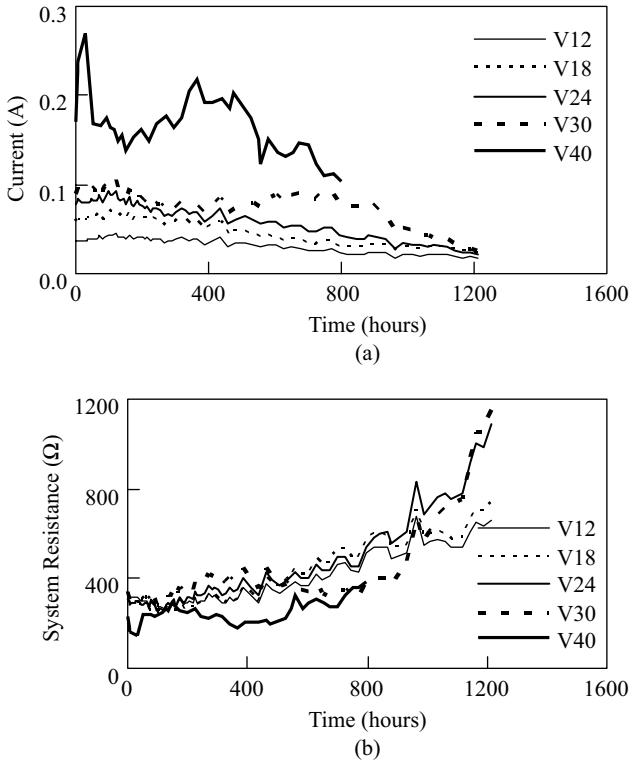

Fig. 4. Changes in (a) current and (b) system resistance during ALMT.

by the hydrated products of cement. The optimum voltage for removing alkalis from the specimen was 18 V, removing 87.4% of alkalis. The increase in the voltage above 18 V has only limited effect on the removal of alkalis.

Figurg 5(a) shows that the average removal rates of Na^+ and K^+ increase with the increase in voltage. However, this relationship is imperfect. But the average removal rates have a

Table 2. Average current densities in different stages during ALMT controlled by constant voltage (Unit: A/m^2).

Experiment #	Initial Experimental Stage (0 ~ 48 h)	Na^+ Removal Stage	K^+ Removal Stage	Li^+ Non-steady State	Li^+ Steady State	Entire Experiment
V12	4.8	4.1	4.5	4.1	2.6	3.9
V18	7.8	6.4	7.5	6.5	3.7	5.7
V24	10.3	9.0	9.5	8.5	5.6	7.1
V30	11.9	10.7	11.1	10.7	10.0	9.4
V40	26.9	20.8	21.4	21.4	22.2	21.8

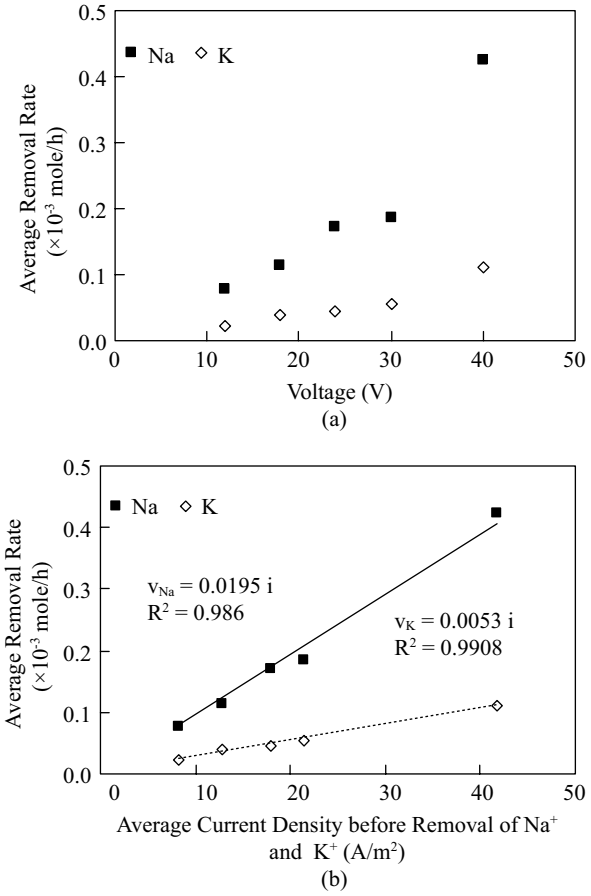

Fig. 5. Relationship between the average removal rate of Na^+ and K^+ and (a) the voltage and (b) the average current density.

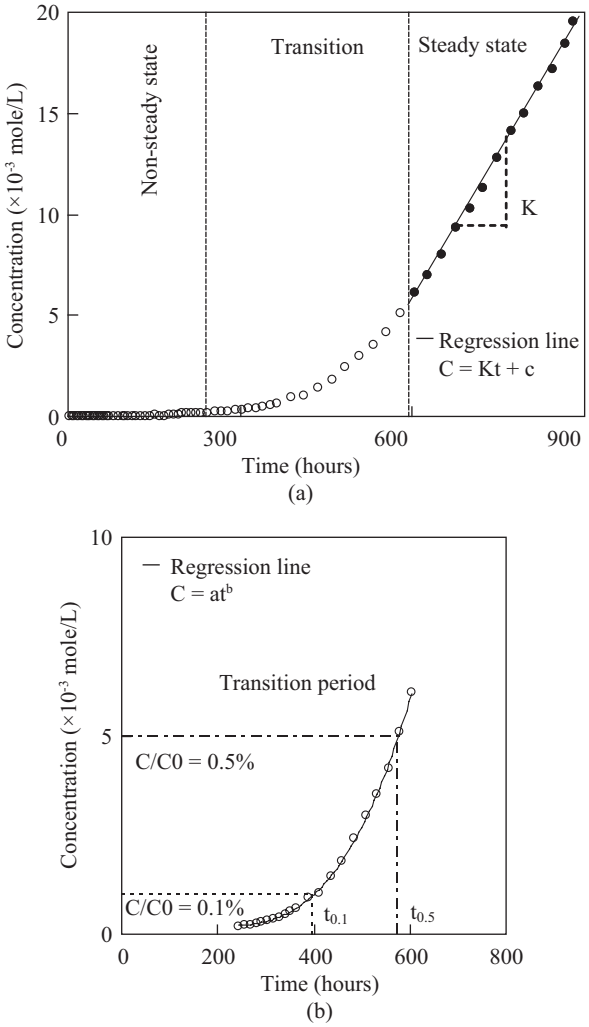

Fig. 6. (a) Changes in Li^+ concentration in catholyte and (b) changes of concentration during transitional stage, for the case of V30.

good linear relationship with the average current density during the removal period of Na^+ and K^+, as shown in Fig. 5(b). Therefore, in the following discussion we will analyze, the relationship between the ion migration parameter and the average current density. The average current densities in different stages during the ALMT process are listed in Table 2.

4. The Migration Behavior of Li^+

During the non-steady state, Li^+ has not yet reached the cathodic cell. Theoretically, the calculation of the non-steady-state migration coefficient uses the actual time that Li^+ takes to pass through the specimen. However, Li^+ in the cathodic cell was not measured continuously, making the time required for Li^+ to pass through the specimen difficult to determine. Therefore, as shown in Fig. 6(b), the regression line for the Li^+ concentration-time curve during the transitional stage was produced as Eq. (1). It can be used to determine the time required for Li^+ to pass through the specimen:

Table 3. The migration coefficients of Li^+ during non-steady state and steady state.

Experiment #	Non-steady State		Steady State		D_s/D_n (%)
	$t_{0.1}$ (h)	D_n ($\times10^{-12}$ m^2/s)	J_s ($\times10^{-7}$ mole/m^2/s)	D_s ($\times10^{-14}$ m^2/s)	
V12	485.8	2.49	1.63	1.78	0.7
V18	386.5	2.23	4.84	3.51	1.6
V24	342.3	2.14	9.30	5.03	2.4
V30	311.2	1.68	18.68	8.10	4.8
V40	143.2	2.82	63.77	20.97	7.4

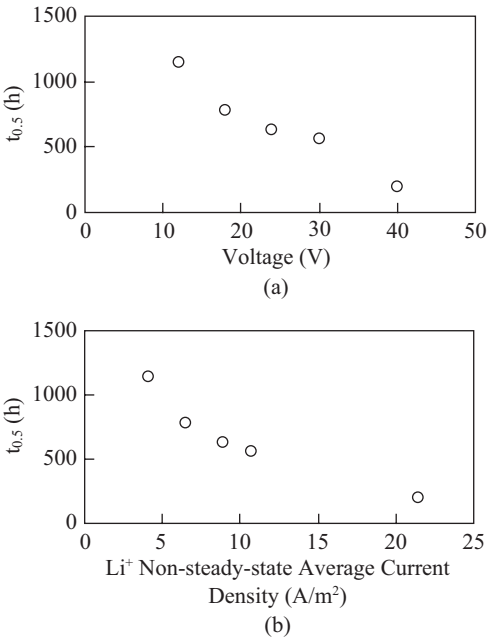

Fig. 7. Relationships between $t_{0.1}$ and (a) voltage and between $t_{0.1}$ and (b) average current density during non-steady state.

$$C = at^b, \text{ for the transitional stage} \quad (1)$$

where C is the Li^+ concentration (mole/L) in the cathodic cell, t is the time for the electrochemical process (s), and a and b are experimental constants. As research on Cl^- migration [5, 16], this study tries to calculate the time ($t_{0.1}$) corresponding to $C/C_0 = 0.1\%$, where C/C_0 is the ratio of Li^+ concentration in a cathodic cell to Li^+ concentration in an anodic cell, as the time required for Li^+ to pass through the specimen. The results are shown in Table 3. Figure 7 shows that the time $t_{0.1}$ will decrease with the increase in the applied voltage or the average current density during the non-steady state. The $t_{0.1}$ has a better correlation with the average current density than the applied constant voltage.

During the steady state, the regression line for the curve, shown in Fig. 6(a), was produced as Eq. (2).

$$C = Kt + c \text{ for the steady state} \quad (2)$$

where K (mole/L/s) is the Li^+ migration rate, the slope of the linear portion of the Li^+ concentration-time curve. It was found that after the removal of Na^+, the migration of Li^+ begins to enter the steady state. While calculating the Li^+ steady-state migration rate, the removal time of Na^+ was used as the beginning of Li^+ steady-state migration. The steady-state flux (J_s) of Li^+ can be calculated as a steady-state migration rate (K) × catholyte volume/specimen cross-section area. The results are shown in Table 3. The steady-state flux increases with the increase in the applied voltage.

5. Migration Coefficient of Li^+ during Non-steady State

The non-steady-state migration coefficient of Li^+, D_n(m^2/s), can be calculated by using the modified Fick's second law [15, 17]:

$$\frac{dC}{dt} = D_n\left(\frac{d^2C}{dx^2} - \frac{|z|FE}{RT}\frac{dC}{dx}\right) \quad (3)$$

where C (mole/L) is the concentration of ions in the cathodic cell, z is the electrical charge of Li^+, F is the Faraday constant (96500 C/mole), E is the strength of the electrical field between the anode and cathode (V/m), R is the universal gas constant (8.31 J/mole/K), and T is the absolute temperature (K). The initial condition is C = 0 for x > 0, t = 0; the boundary condition is $C = C_0$ for x = 0, t > 0; and C = 0 for x = infinite, t = large number. The analytical solution for Eq. (3) is given by:

$$C(x,t) = \frac{C_0}{2}\left[e^{\alpha x}erfc\left(\frac{x + aD_nt}{2\sqrt{D_nt}}\right) + erfc\left(\frac{x - aD_nt}{2\sqrt{D_nt}}\right)\right] \quad (4)$$

where $a = \frac{|z|FE}{RT}$, C_0 is the Li^+ concentration (mole/L) in the anodic cell, and erfc is the complementary error function.

From Eq. (4), D_n can be calculated as:

$$D_n = \frac{1}{a}\left[\frac{x - \alpha\sqrt{x}}{t}\right] \quad (5)$$

where $\alpha = 2\sqrt{\frac{1}{a}} erf^{-1}(1-\frac{2C}{C_0})$, and erf^{-1} is the inverse of the error function.

Use $t_{0.1}$ as the time needed for Li^+ to pass through the specimen. The non-steady-state migration coefficient D_n can be calculated from Eq. (5) by substituting $t = t_{0.1}$, as shown in Table 3. D_n values are around $1.68 - 12.82 \times 10^{-12}$ m^2/s.

6. Migration Coefficient of Li^+ during Steady State

The general law governing ion transfer in electrolytes is given by the Nernst-Planck equation. There is no velocity of solution during the ALMT experiment, so there is no convection of ions. According to Kropp's research [5], diffusion is negligible compared with migration when the external electrical field applied is higher than 10 V. Thus, the Nernst-Planck equation can be condensed to:

$$J(x) = \frac{Z_j F}{RT} D_j C \frac{\partial E_x}{\partial x} \tag{6}$$

Transposing Eq. (6) gives Eq. (7). Andrade [1] proposed that the solution of the steady-state migration coefficient D_s, m^2/s, of ions within concrete can be obtained by substituting the steady-state flux J_s obtained from the experiment into Eq. (7) [5, 14]:

$$D_s = \frac{J_s RTx}{zFC\Delta E} \tag{7}$$

where J_s is the steady-state flux of ions (mole/m^2/s), x is the distance between electrodes (m), z is the electrical charge of the ions, C is the concentration of upstream ions (mole/m^3), and ΔE is the applied voltage (V). The calculated D_s of the experiments are shown in Table 3.

Figure 8(a) shows that both the steady-state flux J_s and the steady-state migration coefficient D_s of Li^+ increased with the increase of the applied voltage. Furthermore, the increment in J_s and D_s per unit of applied voltage also increased with the increase of the applied voltage. In Fig. 8(b), there exists a positive linear relationship among J_s and D_s and the average current density in a steady-state. Figure 9 also demonstrates a positive linear relationship between J_s and D_s of Li^+.

In field application, the purpose of ASR maintenance has been accomplished when most of Na^+ and K^+ are removed from the concrete. Therefore, the magnitude of J_s and D_s values of Li^+ does not directly affect the outcome of the maintenance. In addition, from Table 3, we see that the migration coefficient D_s is around 0.7-7.4% of D_n. This result shows that some pores might have been blocked during the steady state, thus lower the steady state migration coefficient [15]. This phenomenon corresponds with the observation that the system resistance increases continuously during the ALMT, as shown in Fig. 4(b).

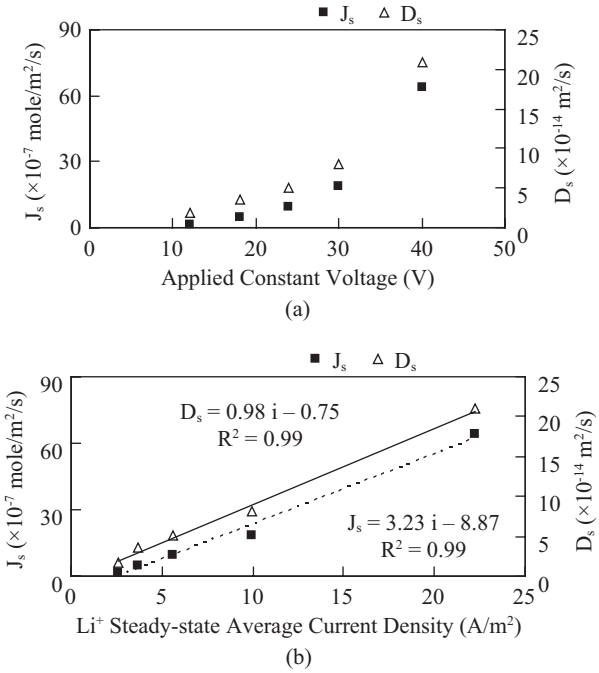

Fig. 8. Relationships among the steady-state flux, migration coefficient of Li^+ and (a) the applied voltage, and among the steady-state flux, migration coefficient of Li^+, and (b) the average current density.

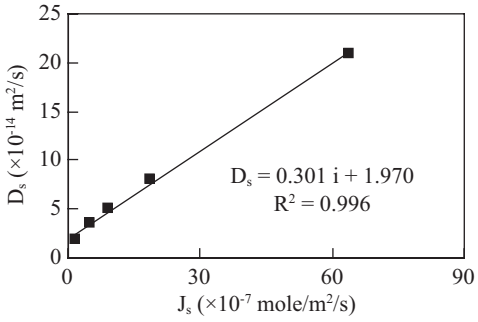

Fig. 9. Relationship between the steady-state flux (J_s) and steady-state migration coefficient (D_s) of Li^+.

The migration rates of Na^+ and K^+, the time for Li^+ to pass through the specimen, J_s and D_s of Li^+, have positive linear relationships with the average current density. However, it is difficult to know the average current density in each migration stage under the applied constant voltage before the field application of ALMT. Therefore, it is difficult to design the applied constant voltage in ALMT application using the current density as an index in advance. But the current density can still act as a tool for monitoring the effectiveness during the ALMT process.

7. Relationship between the Accumulated Applied Charge and the Charge Carried by the Cations

Figure 10 shows the typical relationship between the ac-

Table 4. Accumulated applied charge after the removal of Na^+.

Experiment #	V12	V18	V24	V30	V40
Accumulated Charge (C)	127855	162647	161903	164541	164232

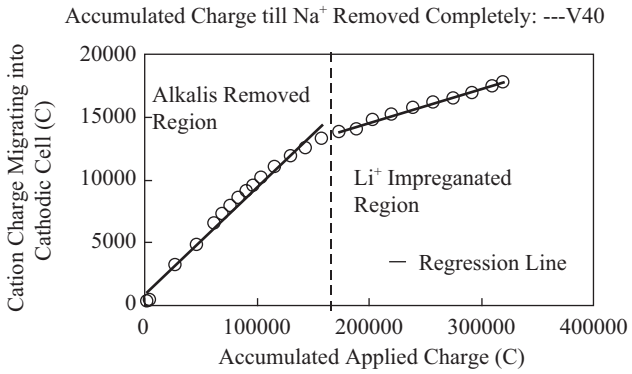

Fig. 10. Typical curve between the charge of cations migrating into the catholyte and the accumulated applied charge.

cumulated charge $\sum Q_{ion}$ of the cations Li^+, Na^+, and K^+ migrating into the cathodic cell and the accumulated applied charge $\sum Q_a$. This relationship between $\sum Q_{ion}$ and $\sum Q_a$ is consistent for every experiment in this study. The $\sum Q_{ion}$ can be calculated as:

$$\sum Q_{ion} = \sum m_i \times F \tag{8}$$

where $\sum m_i$ is the sum of the accumulated molar numbers of Na^+, K^+, and Li^+. $\sum Q_a$ can be obtained as:

$$\sum Q_a = \sum_n I_n \Delta t \tag{9}$$

where I_n is the measured current (A), and Δt is the time difference (s).

The curve in Fig. 10 can be divided into two linear regions. The accumulated charge until Na^+ is removed completely in the experiments, Table 4, is found at the boundary between the two linear regions. Before the boundary, the cations migrating out of the specimen are mainly Na^+ and K^+. This is defined as the alkalis removed region. After most of the Na^+ and K^+ have been removed, the cations migrating out of the specimen are mainly Li^+. This is defined as the Li^+ impregnated region. In Fig. 10, the slope of the alkalis removed region is greater than the slope of Li^+ impregnated region. This also corresponds with the fact that the mobility of Na^+ and K^+ is greater than that of Li^+ under the applied electric field [12].

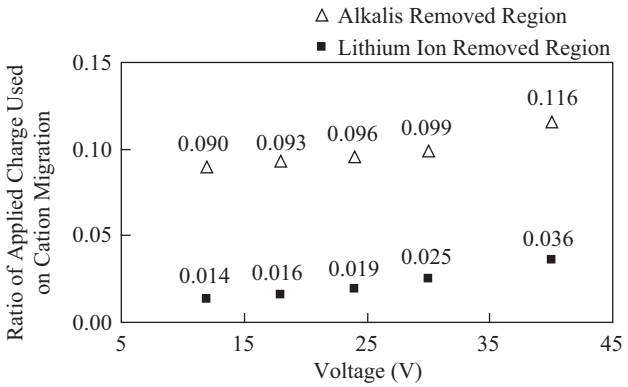

Fig. 11. Relationship between the slopes of the alkalis and the Li^+ removed regions of Fig. 10 curve and the applied voltage.

Furthermore, in Fig. 10, the ratios of the applied charge used for the cation migration are shown in Fig. 11. Only 9.0-11.6% of the applied charge is used for Na^+ and K^+ removal, and 1.4-3.6% of the applied charge is used to impregnate specimens with Li. Since increasing the applied voltage can increase the proportion of the applied charge being used for cation migration, thus it provides better electrical efficiency. This result means that during the field application of the ALMT, a higher voltage is beneficial for driving out the alkalis and impregnating concrete with Li^+.

8. Distribution of Soluble Cations in Specimen after ALMT Process

Limiting the alkali content of cement or the total alkali content of concrete is an easy and effective strategy against ASR damage. ASTM limits the alkali content of cement to under 0.6% Na_2O_{eq}. Furthermore, the limit on the alkali content of concrete is specific to each region, thus, each country has different regulations. Hobbs [4] has pointed out that by using opal as aggregate, the concrete will not expand while its total alkali content is less than 2 kg/m^3.

Figure 12 shows that the free Na^+ and K^+ remaining in the specimen after the ALMT process are both less than 1 kg/m^3, lower than the original content in the specimen (6.80 kg/m^3 and 2.79 kg/m^3, respectively). After conversion into Na_2O_{eq}, the average residue alkali content of all experiments was less than 0.58 kg/m^3, far lower than the total Na_2O_{eq} content before the ALMT process (11.37 kg/m^3).

Figure 12 shows that the free Li^+ content in the specimen after the ALMT process gradually decreases from the anode to the cathode. Since the ALMT process in this research experienced steady-state migration, the concentration distribution of Li^+ in the treated specimen is even. Therefore, an increase in system resistance during the final stages of the ALMT process indicates that the pores structure may be due to congestion.

Furthermore, the average free Li^+ impregnated into the specimen is about 1.12-2.49 kg/m^3 for Experiments V12~V30, while there is little Na^+ and K^+ remaining within the specimen.

Table 5. Molar ratio of free Li/(Na + K) in specimen after the ALMT process.

Experiment #	V12	V18	V24	V30
Li/(Na + K) Molar Ratio	9.6	10.4	19.6	15.5

Note: Data of Experiment V40 has not been included due to its shorter electrochemical process time.

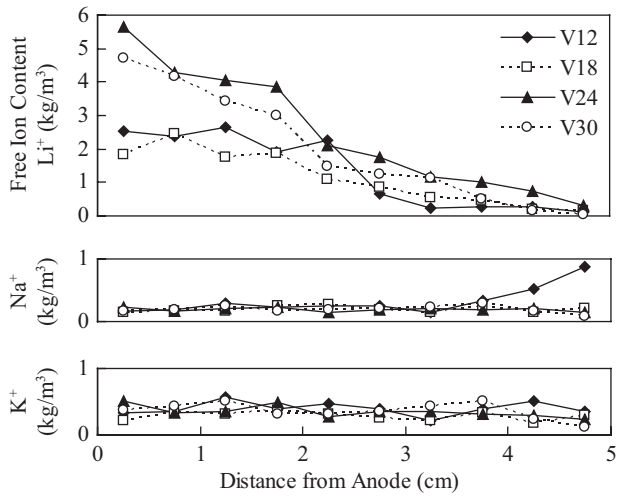

Fig. 12. Free cation content in the specimen after the ALMT process.

As shown in Table 5, the molar ratio of free Li/(Na + K) in the specimen is around 9.6-19.6, which far exceeds the suggested effective inhibiting value of 0.74 [7].

The application of ALMT removes Na^+ and K^+ from concrete and impregnates the specimen with sufficient Li^+ simultaneously. Thus, the ALMT process not only inhibits ASR, but also prevents the occurrence of future ASR caused by the ingress of Na^+ and K^+.

IV. CONCLUSION

The following conclusions are drawn from this research:

1. Four stages for Li^+ migration can be observed from the ALMT process controlled by constant voltage. During the non-steady state, Li^+ has not yet reached the cathodic cell, while Na^+ and K^+ are migrating steadily outside the specimen. The current first increases, then decreases. During the transitional stage, the Li^+ flux gradually increases, and the Na^+ and K^+ flux gradually decreases. After the removal of the alkali content, Li^+ migration enters the steady state. During the steady state, Li^+ flux is stable and the current is maintained within a certain range. During the attenuation stage, the current gradually decreases, while the Li^+ flux also decreases gradually.
2. The average temperature of the ALMT process increases with the increase of applied voltage. When the ALMT process time increases, the current decreases, whereas the system resistance increases.
3. The removal time of K^+ is shorter than that of Na^+. The optimum voltage for effectively removing the most alkalis is around 18V, removing 87.7% alkalis. The increase of voltage greater than 18V has only a limited increase in the removal of alkalis.
4. With the increase of applied voltage, the removal rate and removal amount of the alkali content increase, the removal time of alkalis and the time of Li^+ passing through the specimen decrease, and the non-steady-state and steady-state migration coefficient of Li increase. There also exist positive linear relationships between ion migration parameters and the average current density at corresponding stages. Thus, voltage and average current density are both good indicators of ion migration.
5. For ALMT experiments under different applied voltages, the relationships between the cations accumulated charge migrating into the catholyte and the applied charge are consistent. The relationship curves include the alkalis removed and the Li^+ impregnated linear regions. The accumulated charge until Na^+ is removed completely is found in the boundary between the two regions, and the linear slope of the alkalis removed region is greater than the slope of Li^+ impregnated region. While increasing the applied voltage can increase the proportion of the applied charge being used for cation migration, only 9.0-11.6% of the applied charge is used for Na^+ and K^+ removal, and 1.4-3.6% of the applied charge is used to impregnate a specimen with Li^+.
6. The average free alkali content of all treated specimens is less than 0.58 kg/m^3, and the average free Li^+ impregnated into the specimen is around 1.12-2.49 kg/ m^3. The molar ratio of free Li/(Na + K) in the treated specimen is around 9.6-19.6.

ACKNOWLEDGMENTS

The authors would like to thank the National Science Council of Taiwan for financial support of this research under Contract No. NSC 96-2221-E-008-085-MY3.

REFERENCES

1. Andrade, C., "Calculation of chloride diffusion coefficients in concrete from ionic migration measurements," *Cement and Concrete Research*, Vol. 23, pp. 724-742 (1993).
2. Chen, D. Y., *Fundamental Study Using Electrochemical Technique to Inhibit AAR*, Master Thesis, Department of Civil Engineering, National Central University, ChungLi, Taiwan (1999). (in Chinese)
3. Era, K., Mihara, T., Kaneyoshi, A., and Miyagawa, T., "Controlling effect of lithium nitrite on alkali-aggregate reaction," *Proceeding of the 13th International Conference on Alkali-Aggregate Reaction*, Trondheim, Norway, pp. 71-78 (2008).
4. Hobbs, D. W., *Alkali-Silica Reaction in Concrete*, Thomas Telford, London, p. 135 (1984).
5. Kropp, J. and Hilsdorf, H. K., *Performance Criteria for Concrete Durability*, RILEM REPORT 12, E & FN SPON, London (1995).

6. Liu, C. C., *Identify the Reactivity of Aggregates in Taiwan and Using Electrochemical Techniques to Mitigate Expansion Due to Alkali-Aggregate Reaction in Concrete*, Ph.D. Dissertation, Department of Civil Engineering, National Central University, ChungLi, Taiwan (2003). (in Chinese)
7. Michael, D. A., Thomas, B. F., Kevin, J. F., Jason, H. I., and Yadhira, R., *The Use of Lithium to Prevent or Mitigate Alkali-Silica Reaction in Concrete Pavements and Structures*, Federal Highway Administration, U.S. Department Transportation, FHWA-HRT-06-133, McLean, VA (2007).
8. Page, C. L. and Yu, S. W., "Potential effects of electrochemical desalination of concrete on alkali-silica reaction," *Magazine of Concrete Research*, Vol. 47, No, 170, pp. 23-31 (1995).
9. Sakaguchi, Y., Takakura, M., and Kitagawa, A., "The inhibiting effect of lithium compounds on alkali-silica reaction," *Proceeding of the 8th International Conference on Alkali-Aggregate Reaction*, Kyoto, pp. 229-234 (1989).
10. Stokes, D. B., "Use of lithium to combat alkali silica reactivity," *Proceeding of the 10th International Conference on Alkali-Aggregate Reaction*, Melbourne, Australia, pp. 862-867 (1996).
11. Thomas, M. D. A., Hooper, R., and Stokes, D., "Use of lithium-containing compounds to control expansion in concrete due to alkali-silica reaction," *Proceeding of the 11th International Conference on Alkali-Aggregate Reaction*, Quebec, Canada, pp. 783-792 (2000).
12. Tian, F. Z., *Electrochemistry: Basic Principle and Application*, Five Continents Publishing House, Taipei, p. 23 (1999). (in Chinese)
13. Whitmore, D. and Abbott, S., "Use of an applied electric field to drive lithium ions into alkali-silica reactive structures," *Proceeding of the 11th International Conference on Alkali-Aggregate Reaction*, Quebec, Canada, pp. 1089-1098 (2000).
14. Yang, C. C., "On the relationship between pore structure and chloride diffusivity from accelerated chloride migration test in cement-based materials," *Cement and Concrete Research*, Vol. 36, pp. 1304-1311 (2006).
15. Yang, C. C. and Chiang, C. T., "On the relationship between pore structure and charge passed from RCPT in mineral-free cement-based materials," *Materials Chemistry and Physics*, Vol. 93, No. 1, pp. 202-207 (2005).
16. Yang, C. C. and Cho, S. W., "An electrochemical method for accelerated chloride migration test of diffusion coefficient in cement-based materials," *Materials Chemistry and Physics*, Vol. 81, pp. 116-125 (2003).
17. Yang, C. C., Cho, S. W., Chi, J. M., and Huang, R., "An electrochemical method for accelerated chloride migration test in cement-based materials," *Materials Chemistry and Physics*, Vol. 77, No. 2, pp. 461-469 (2003).